BIOCHEMISTRY
including biophysical chemistry & molecular biology
Article

*Biochemistry* **2010,** *49,* 5909–5918 5909
DOI: 10.1021/bi100748s

# Amino Acid Sequence Requirements of Laminin $\beta$1 Chain Peptide B133 (DISTKYFQMSLE) for Amyloid-like Fibril Formation, Syndecan Binding, and Neurite Outgrowth Promotion

Fumihiko Katagiri,[‡] Kazuki Takeyama,[‡] Yukiko Ohga,[‡] Kentaro Hozumi,[‡] Yamato Kikkawa,[‡] Yuichi Kadoya,[§] and Motoyoshi Nomizu*[,‡]

[‡]*Laboratory of Clinical Biochemistry, School of Pharmacy, Tokyo University of Pharmacy and Life Sciences, 1432-1 Horinouchi, Hachioji, Tokyo 192-0392, Japan, and* [§]*Department of Anatomy, Kitasato University School of Allied Health Sciences, Sagamihara, Kanagawa 228-8555, Japan*

*Received May 12, 2010; Revised Manuscript Received June 14, 2010*

ABSTRACT: Peptide B133 (DSITKYFQMSLE), derived from mouse laminin $\beta$1 chain (residues 1298−1309), promotes cell attachment, neurite outgrowth, and amyloid-like fibril formation. Previously, we showed that the N-terminal Asp-deleted peptide B133a (SITKYFQMSLE) promotes integrin $\alpha 2\beta 1$-mediated cell attachment and spreading but does not form amyloid-like fibrils, and that the C-terminal Glu-deleted peptide B133g (DSITKYFQMSL) attaches cells without cell spreading and forms amyloid-like fibrils. In this study, we further investigated the amino acid sequence requirements of B133 for biological function using a set of truncated and Ala-substituted peptides. Attachment of cells to B133g was inhibited by only heparin, and Congo Red analysis indicated that the amyloid-like fibril formation activity of B133g was stronger than that of B133. Alanine scan analysis for the B133g peptide indicated that Asp and Ile residues are essential for cell attachment. Additionally, the N-terminal Asp residue was required for neurite outgrowth. Further, amyloid-like fibril formation required Asp and Ile residues. These data suggest that the amyloid-like fibril formation of B133g is required for cell attachment activity. We also evaluated the attachment of cells to the peptides using syndecan- and glypican-overexpressing cells. B133g attached to syndecan-overexpressing cells but not to glypican-overexpressing cells, suggesting that the amyloidogenic peptides promote syndecan-mediated cell attachment. These findings were useful for clarifying the mechanism of amyloid-like fibril formation and biological functions. The B133 peptide promotes amyloid-like fibril formation, syndecan-mediated cell attachment, and neurite outgrowth and has the potential for use as a biomaterial for tissue engineering.

Amyloid fibrils are insoluble fibrils 7−10 nm in diameter with a cross-$\beta$ structure. These fibrils form highly axially aligned $\beta$ strands by hydrogen bonds. Amyloid fibrils exhibit a red to green birefringence after being stained with Congo Red (*1*, *2*), and a characteristic UV absorbing spectrum at the peak of 540 nm with Congo Red (*3*−*5*). The process of amyloid fibril formation is associated with several diseases, including Alzheimer's disease, Parkinson's disease, type II diabetes, prion diseases, and systemic polyneuropathies (*6*, *7*). Although amyloid fibril formation is generally associated with disease processes, many proteins not associated with amyloid-related diseases can also form amyloid-like fibrils (*8*−*10*). Amyloid fibril formation is different from the simple process of nonspecific aggregation because it has ordered structures that possess a characteristic X-ray diffraction pattern (*11*, *12*). Thus, a specific pattern of molecular interactions, rather than nonspecific hydrophobic interactions, leads to ordered structures. Common structural elements responsible for such organized structures have not been identified.

Previously, we reported that several cell-adhesive peptides derived from laminin form amyloid-like fibrils (*5*). Laminins are major components of basement membrane extracellular matrices and play a critical role in the biological functions of basement membranes (*13*). Laminins are trimeric molecules composed of $\alpha$, $\beta$, and $\gamma$ chains, and so far, five $\alpha$, three $\beta$, and three $\gamma$ chains have been identified. Laminin-111 ($\alpha 1\beta 1\gamma 1$) has diverse biological activities, including promotion of cell adhesion and neurite outgrowth (*13*). The Ile-Lys-Val-Ala-Val (IKVAV) sequence derived from the laminin $\alpha$1 chain promotes neurite outgrowth via interaction with a 110 kDa membrane-associated laminin-binding protein from brain (*14*), and the membrane protein has been identified as a $\beta$-amyloid precursor protein (*15*, *16*). The IKVAV-containing peptides form amyloid-like fibrils, and the structure is critical for biological activity. We have also reported that peptide B133 (DSITKYFQMSLE, mouse laminin $\beta$1 chain residues 1298−1309) promotes integrin $\alpha 2\beta 1$-mediated cell attachment, neurite outgrowth, and amyloid-like fibril formation (*5*). The N-terminal Asp-deleted peptide B133a (SITKYFQMSLE) exhibited integrin $\alpha 2\beta 1$-mediated cell attachment, although amyloid-like fibril formation and neurite outgrowth activity were eliminated (*17*). In contrast, the C-terminal Glu-deleted peptide B133g (DSITKYFQMSL) promoted a heparin-dependent cell attachment and amyloid-like fibril formation (*17*). The cell attachment mechanism of amyloidogenic peptides, including B133g, is not well understood yet.

Here, we focused on the B133 peptide and evaluated sequential requirements for amyloid-like fibril formation and biological

*To whom correspondence should be addressed: Tokyo University of Pharmacy and Life Sciences, 1432-1 Horinouchi, Hachioji, Tokyo 192-0392, Japan. Phone and fax: 81-426-76-5662. E-mail: nomizu@toyaku.ac.jp.


Published on Web 06/15/2010

activity, including cell attachment and neurite outgrowth, using a set of amino acid deletion and Ala substitution peptides. We also evaluated the cellular receptors for the B133-related peptides.

## MATERIALS AND METHODS

*Synthetic Peptides*. All peptides were prepared manually by the 9-fluorenylmethyloxycarbonyl (Fmoc)-based solid-phase synthesis with a C-terminal amide as described previously (*18*). The respective amino acids were condensed manually in a stepwise manner using diisopropylcarbodiimide *N*-hydroxybenzotriazole on a 4-(2′,4′-dimethoxyphenyl-Fmoc-aminomethyl)-phenoxy resin (Rink amide resin, Novabiochem, San Diego, CA). Resulting protected peptide resins were deprotected and cleaved from the resin using a trifluoroacetic acid (TFA)/thioanisole/*m*-cresol/ethanedithiol/$H_2O$ mixture (80:5:5:5:5, v/v) at 20 °C for 3 h. Crude peptides were precipitated and washed with diethyl ether and then purified by high-performance liquid chromatography (HPLC)[1] using a Mightysil RP-18 column (Kanto Chemical Co., Inc., Tokyo, Japan) with a gradient of $H_2O$ and acetonitrile containing 0.1% TFA. The purity and identity of the synthetic peptides were confirmed by HPLC and by electrospray ionization mass spectroscopy. Mass spectroscopy was performed at the Central Analysis Center, Tokyo University of Pharmacy and Life Sciences. Peptides were dissolved in water at 1 mg/mL, kept at 4 °C for 1 week, and then used for the assay.

*Congo Red Binding Analysis*. A 100 μM stock solution of Congo Red was prepared in phosphate-buffered saline (PBS) and 10% ethanol (*3*). Ethanol was added to prevent the formation of Congo Red micelles. This Congo Red stock solution was filtered three times using a 0.45 Micron Nylon Membrane (AGC techno glass Co. Ltd., Chiba, Japan).

The peptide solutions in water (100 μL, dissolved at a final concentration of 0.1 mg/mL) and the Congo Red stock solution (100 μL) were mixed with 800 μL of PBS (1.25×) and incubated in disposable cuvettes for 24 h at room temperature. Absorption spectra were recorded from 300 to 700 nm using a UV-1700 UV−vis spectrophotometer (Shimadzu Co. Ltd., Kyoto, Japan).

*Congo Red Staining and Polarized Light Microscopy*. Peptides were dissolved in water at a concentration of 5 mg/mL, and the solution was pipetted onto a glass slide. After being dried overnight, the precipitate was stained with a 1% aqueous solution of Congo Red for 1 h. After being rinsed with pure acetone, the samples were dehydrated with 95% ethanol and 100% ethanol and then cleared with xylene. The specimens were mounted with a resin (malinol, Muto Pure Chemicals, Tokyo, Japan) and observed in a microscope (AX80, Olympus, Tokyo, Japan) either under bright field illumination or between crossed polars.

*Electron Microscopy*. A peptide solution (1 mg/mL) was diluted 2-fold with water and applied onto a grid mesh with carbon-coated Formvar film [0.5% ethylene dichloride solution of polyvinyl formal (Nisshin EM Co. Ltd., Tokyo, Japan)]. The specimen was then negatively stained with a 1.5% aqueous solution of uranyl acetate and observed using a JEM-1011 (JEOL Ltd., Tokyo, Japan) electron microscope at an acceleration voltage of 80 kV.

[1]Abbreviations: Fmoc, 9-fluorenylmethyloxycarbonyl; HPLC, high-performance liquid chromatography; PBS, phosphate-buffered saline; DMEM, Dulbecco's modified Eagle's medium; FBS, fetal bovine serum; BSA, bovine serum albumin; EDTA, *N*,*N*,*N*′,*N*′-ethylenediaminetetraacetic acid; NGF, nerve growth factor.

*Cells and Culture*. A human fibrosarcoma cell line [HT1080 cells (HSRRB, Osaka, Japan)] was maintained in Dulbecco's modified Eagle's medium [DMEM (Wako Pure Chemical Industries, Ltd., Osaka, Japan)], containing 10% fetal bovine serum (FBS), 100 units/mL penicillin, and 100 μg/mL streptomycin (Invitrogen, Carlsbad, CA). Rat pheochromocytoma PC12 cells (*19*) were maintained in DMEM containing 7.5% horse serum, 7.5% FBS, 100 units/mL penicillin, and 100 μg/mL streptomycin. The series of human ARH-77 B-lymphoid cell lines, which are transfected with heparan sulfate proteoglycans (syndecan-1, -2, and -4 and glypican-1) (*20*−*22*), were grown in suspension in RPMI-1640 medium (Wako) supplemented with 5% FBS, 100 units/mL penicillin, and 100 μg/mL streptomycin. All cells were maintained at 37 °C in a humidified 5% $CO_2$/95% air atmosphere.

*Cell Attachment Assay Using Peptide-Coated Plates*. The attachment of cells to peptide-coated plates was assayed in 96-well plates (Nunc, Inc., Naperville, IL). Plates were coated with various amounts of peptide in water and dried overnight. The peptide-coated wells were blocked with 1% bovine serum albumin [BSA (Sigma, St. Louis, MO)] in DMEM (150 μL) for 1 h and then washed twice with DMEM containing 0.1% BSA. Cells were detached with trypsin and *N*,*N*,*N*′,*N*′-ethylenediaminetetraacetic acid (EDTA), resuspended in DMEM containing 0.1% BSA, were added to each well (20000 cells/100 μL), and incubated at 37 °C for 1 h in 5% $CO_2$. The attached cells were stained with a 0.2% crystal violet aqueous solution in 20% methanol for 10 min. After being washed with water, the attached cells were photographed using a BZ-8000 microscope (Keyence, Osaka, Japan). Images were captured and analyzed using BZ-analyzer (Keyence). The attached cells in three randomly selected fields (0.67 $mm^2$) were counted. All assays were conducted in triplicate, and each experiment was repeated at least three times.

*Inhibition Assay*. For inhibition of the attachment of cells to peptide-coated plates, 96-well plates (Nunc) were coated with peptides as described above. The cells were preincubated for 15 min at room temperature in the presence of either 10 μg/mL heparin or 5 mM EDTA prior to being plated in the wells. HT1080 cells (20000 cells per 100 μL per well) were added to the wells and incubated at 37 °C in 5% $CO_2$ for 30 min. After being stained with 0.2% crystal violet in 20% methanol for 15 min, the attached cells were counted under the BZ-8000 microscope.

*Neurite Outgrowth*. For the neurite outgrowth assay, 96-well plates (Nunc) were coated with various amounts of peptides and dried for overnight. The peptide-coated plates were washed with DMEM/F12 (Invitrogen). PC12 cells were primed with 100 ng/mL nerve growth factor [NGF (Roche Diagnostics GmbH, Mannheim, Germany)] for 24 h prior to the assay. The PC12 cells were then released from the dish by agitation, collected by centrifugation, allowed to recover in culture medium for 30 min at 37 °C in 5% $CO_2$, and then washed three times with DMEM/F12. After being washed, cells were resuspended in DMEM/F12 containing 100 μg/mL transferrin (Sigma), 20 nM progesterone (Sigma), 30 nM $Na_2SeO_3$ (Wako), 5 μg/mL insulin (Invitrogen), and 100 ng/mL NGF. The cells (5000 cells per 100 μL per well) were added to 96-well plates. After incubation at 37 °C for 24 h in 5% $CO_2$, the cells were fixed with 20% formalin and then stained with 0.2% crystal violet. After being washed with water, the attached cells were photographed using a BZ-8000 microscope (Keyence). Images were captured and analyzed using BZ-analyzer (Keyence). In each well (three fields), 100 cells were viewed,

Table 1: Biological Activities of B133 and Its Truncated Derivatives

| Peptide | Sequence | Congo red binding analysis[a] | Amyloid-like fibril formation | Cell attachment | | Neurite outgrowth[c] |
|---|---|---|---|---|---|---|
| | | | | HT1080[b] | HDF* | |
| Aβ22-35 | EDVGSNKGAIIGLM | +++ | + | + | + | + |
| A208 | AASIKVAVSADR | +++ | + | ++ | + | + |
| B133 | DSITKYFQMSLE | ++ | + | ++ | + | + |
| B133a | SITKYFQMSLE | − | − | + | + | − |
| B133b | ITKYFQMSLE | − | − | + | + | − |
| B133c | TKYFQMSLE | − | − | ++ | + | − |
| B133d | KYFQMSLE | − | − | ++ | + | + |
| B133e | YFQMSLE | − | − | − | − | + |
| B133f | FQMSLE | − | − | − | − | − |
| B133g | DSITKAFQMSL | +++ | + | ++ | + | ++ |
| B133h | DSITKYAQMS | ++ | + | ++ | + | ++ |
| B133i | DSITKYFAM | + | + | ++ | + | ++ |
| B133j | DSITKYFQ | − | − | ++ | + | − |
| B133k | DSITKYF | − | − | − | − | − |
| B133l | DSITKY | − | − | − | − | − |
| AG73 | RKRLQVQLSIRT | − | − | ++ | + | ++ |
| AG73T | LQQRRSVLRTKI | − | − | − | − | − |

[a]Peptides were incubated with a Congo Red solution, and the absorption spectrum at 540 nm was evaluated on the following subjective scale: +++, strong spectrum compared to that of B133; ++, spectrum comparable to that of B133; +, weak spectrum compared to that of B133; −, no shift in the absorption peak. [b]The attachment of cells to peptides was scored on the following subjective scale: ++, activity comparable to that on AG73; +, weak activity compared with that on AG73; −, inactive. [c]Neurite outgrowth of PC12 cells was scored on the following subjective scale: ++, promote neurite outgrowth; +, promote neurite outgrowth only at a high concentration; −, inactive. *Data from ref *17*.

and the percent that had neurites that extended two times the cell diameter in length or longer was determined and averaged for each peptide amount tested.

*Statistical Analysis*. Results are expressed ± the standard error (SE). Comparison of mean values was performed using one-way analysis of variance, and a homoscedastic *t* test. $P < 0.01$ indicated statistical significance.

## RESULTS

*Congo Red Staining and Polarized Microscopy Analysis of Truncated B133 Peptides*. Previously, we reported that the B133 peptide (DSITKYFQMSLE, mouse laminin β1 chain residues 1319−1330) forms amyloid-like fibrils and promotes cell attachment and spreading (*5*, *23*). Deletion analysis of B133 showed that the nine N-terminal residues (B133i, DSITKYFQM) are critical for amyloid-like fibril formation and heparin-dependent cell attachment, and that the eight C-terminal residues (B133d, KYFQMSLE) make up a minimum active sequence for integrin α2β1-mediated cell attachment (*17*). Here, we further evaluated the sequential requirements of B133 for amyloid-like fibril formation and for biological function using systematic truncated peptides (Table 1).

First, we evaluated the effect of B133 and its C-terminally truncated peptides on the Congo Red absorption spectrum. We used Aβ22−35 (EDVGSNKGAIIGLM, β-amyloid protein residues 22−35) (*24*, *25*) and laminin-derived peptide A208 (AASIKVAVSADR, mouse laminin α1 chain residues 2097−2108) (*18*) as controls (Figure 1A). When the Congo Red solution was incubated with B133g, B133h, and B133i, the Congo Red absorption peak was shifted at 540 nm in a manner similar to that of the two positive controls, Aβ22−35 and A208 (Figure 1A). In contrast, B133j did not influence the Congo red absorption. B133g displayed the strongest absorption feature (Figure 1A), suggesting that the N-terminal Asp is important for amyloid-like fibril formation.

We also examined the birefringence of Congo Red-stained B133, B133g, B133h, and B133i peptides using polarized microscopy. The Congo Red-stained Aβ22−35 peptide exhibited the red to green birefringence as expected (*5*) (Figure 1B). The peptides all exhibited red to green birefringence as well as that of Aβ22−35 (Figure 1B). These results suggest that the B133, B133g, B133h, and B133i peptides form amyloid-like fibrils and significantly bound to Congo Red.

*Attachment of Cells to Truncated B133 Peptides*. Next, we examined the cell attachment activity of B133 and its truncated peptides using HT-1080 human fibrosarcoma cells (Figure 2 and Table 1). AG73 (RKRLQVQLSIRT, mouse laminin α1 chain residues 2719−2730) and AG73T (LQQRRSVLRTKI, scramble of AG73) were used as positive and negative controls, respectively (*26*). AG73 has strong cell attachment activity and binds heparin and syndecans, a membrane-associated heparan sulfate proteoglycan (*27*−*29*). B133, B133a−d, and B133g−j exhibited HT1080 cell attachment activity in a dose-dependent manner, but the rest of the truncated peptides did not exhibit activity (Figure 2). B133k (DSITKYF) exhibited slight cell attachment at the small peptide dose (< 1 μg/well) and cell

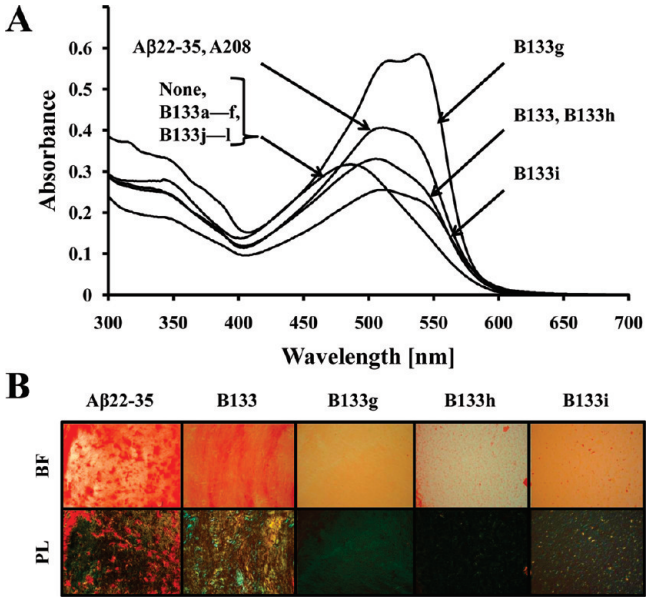


FIGURE 1: Absorption spectra (A) and photomicrographs (B) of peptides stained with Congo Red. (A) Peptide dissolved in water (100 $\mu$L, 1.0 mg/mL) and a Congo Red solution (100 $\mu$L, 100 $\mu$M in PBS) were mixed with 800 $\mu$L of PBS (1.25×) and incubated for 24 h at room temperature. Absorption spectra were recorded from 300 to 700 nm. (B) Peptides in water (5 mg/mL) were pipetted onto a glass slide. After the mixtures had been dried overnight, the precipitate was stained with a 1% aqueous solution of Congo Red for 1 h. After being rinsed with pure acetone, the samples were dehydrated with 95% ethanol and with 100% ethanol and then cleared with xylene. The specimens were mounted with a resin and observed in a microscope either under bright field (BF) illumination (top row) or between crossed polarized light (PL, bottom row).

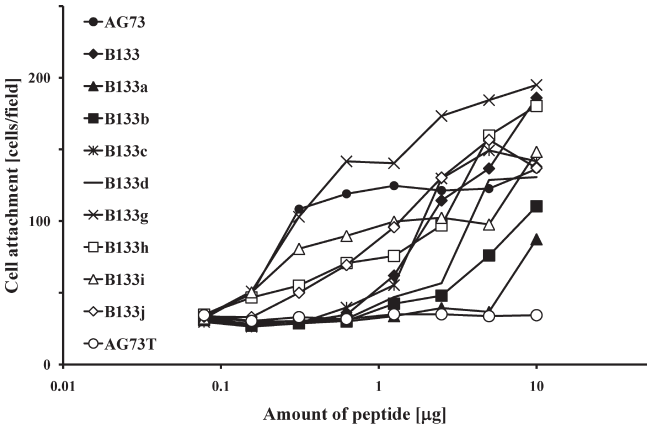


FIGURE 2: Cell attachment activity of B133 and its truncated peptides. Ninety-six-well plates were coated with various amounts of peptides, and HT-1080 cells were added. After a 1 h incubation, the number of attached cells was assessed by crystal violet staining. Data are expressed as the mean of triplicate results. AG73 and AG73T were used as positive and negative controls, respectively.

toxicity at higher doses, but the cell attachment activity was not significant (Table 1). C-Terminally truncated peptides B133a−d exhibited lower HT1080 cell attachment activity than N-terminally truncated peptides B133g−j (Figure 2).

*Effect of EDTA and Heparin on the Attachment of HT1080 Cells to Peptides*. We examined the effect of EDTA and heparin on the attachment of HT1080 cells to the peptides (Figure 3). AG73 and EF1 (DYATLQLQEGRLHFMFDLG, mouse laminin α1 chain residues 2747−2765) (*30*) were used as positive controls. AG73 promotes a syndecan-mediated cell attachment and was inhibited by only heparin as shown previously (*26*). EF1 promotes an integrin α2$\beta$1-mediated cell attachment and was inhibited by only EDTA (*30*). Both EDTA and heparin significantly inhibited the attachment of cells to B133, suggesting that B133 promotes both integrin-mediated and heparan sulfate proteoglycan-mediated cell attachment as shown previously (*5*, *17*) (Figure 3). The attachment of HT1080 cells to B133g−j was inhibited by heparin and was not inhibited by EDTA (Figure 3). These results suggest that HT1080 cells bind to B133g−j through heparin-dependent molecules, including heparan sulfate proteoglycans. In contrast, the attachment of HT1080 cells to the B133a−d peptides was not inhibited by either EDTA or heparin (data not shown). Fibroblast attached to B133a−d peptides was previously described to be inhibited by EDTA and anti-integrin α2 and $\beta$1 antibodies (*17*). The discrepancy may be due to the cell type, but the exact mechanism is not clear at this time.

*Binding of B133 and Its Derivatives to Syndecan-1-, -2-, and -4-Overexpressing and to Glypican-1-Overexpressing Lymphoid Cells*. The attachment of cells to B133 and its N-terminally truncated peptides strongly promoted heparin-dependent HT1080 cell attachment. Binding of the B133 and its derivatives (B133a and -g) to syndecans and glypican-1, which are heparan sulfate proteoglycans, was examined using syndecan-1-, -2-, and -4-overexpressing and glypican-1-overexpressing ARH-77 B-lymphoid cells (Figure 4) (*20*−*22*). ARH-77 cells express small amounts of cell surface heparan sulfate. AG73, A$\beta$22−35, and A208 were used as controls. ARH-77 cells attached to only peptide A208. The A208 peptide containing the IKVAV sequence also promoted the attachment of syndecan-expressing cells equal to ARH-77 cells. IKVAV-containing peptides bind to the 110 kDa amyloid precursor protein (*16*). B133, B133g, B133h, and B133i bound to the all syndecan-overexpressing cell lines but did not bind to the glypican-1-expressing cell lines (Figure 4). These results suggest that syndecans are critical for the attachment of cells to B133 and the N-terminally truncated active peptides. The C-terminal Asp-deleted peptide, B133a, did not promote attachment to the heparan sulfate proteoglycan-overexpressing cells. The B133a peptide did not form amyloid-like fibrils and promoted integrin α2$\beta$1-mediated cell attachment (*17*, *31*). The C-terminal Asp residue is likely critical for syndecan binding. The A$\beta$22−35 peptides also attached to syndecan-overexpressing cells specifically. We conclude that certain types of amyloid-like fibrils may exhibit syndecan-mediated cell attachment.

*Effect of Truncated B133 Peptides on Neurite Outgrowth*. Next, we evaluated the neurite outgrowth activity of the truncated B133 peptides (B133a−l) (Figure 5). We reported previously that the amyloid-like fibril-forming peptides had neurite outgrowth activity (*5*). Neurite outgrowth of PC12 cells was stimulated on B133, B133g, B133h, and B133i, but it was weak on B133h. In addition, B133g−i stimulated neurite outgrowth with a smaller amount of peptide (10 $\mu$g/mL) compared to that required by B133 (50 $\mu$g/mL). The N-terminally truncated peptides (B133a−f) and the short C-terminally truncated peptides (B133i−l) did not stimulate neurite outgrowth. Morphological differences were not observed among the A$\beta$22−35, A208, and B133-derived peptides (Figure 5B).

*Effect of Alanine-Substituted B133g Peptides on the Congo Red Absorption Spectrum*. B133g exhibited the strongest activity for Congo Red staining, amyloid-like fibril formation, HT1080 cell attachment, and neurite outgrowth promotion.

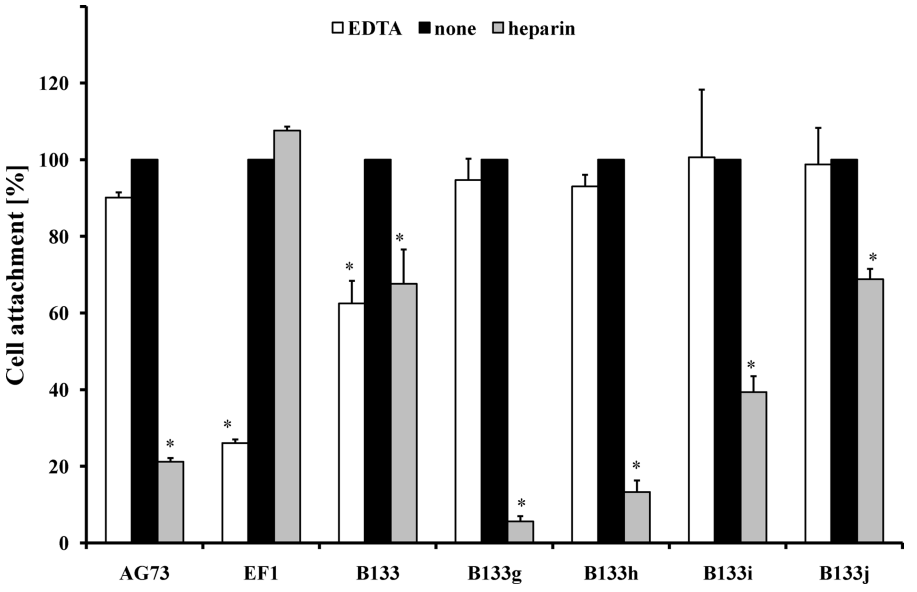


FIGURE 3: Effects of EDTA and heparin on the attachment of HDF to B133 and B133 truncated peptides (B133g−j). Ninety-six-well plates were coated with 5 $\mu$g of peptides. HT1080 cell suspensions were preincubated with either 5 mM EDTA or 10 $\mu$g/mL heparin. Then, the cells were added and incubated. After a 30 min incubation, the number of attached cells was assessed by crystal violet staining. Data are expressed as the mean ± SE of triplicate results. *$P < 0.01$ vs none.

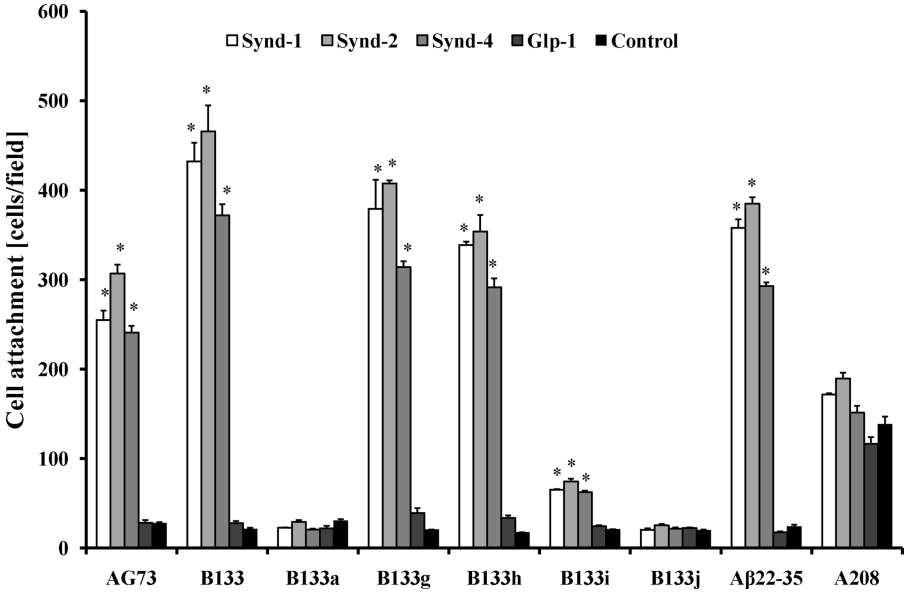


FIGURE 4: Cell attachment activity of the amyloidogenic peptides with various heparan sulfate cell surface receptor-overexpressing cell lines. Heparan sulfate cell surface receptor-overexpressing cell lines with syndecan-1 (Synd-1), syndecan-2 (Synd-2), syndecan-4 (Synd-4), and glypican-1 (Glp-1) and controls without these receptors (control) were used. Each peptide was coated on a 96-well plate. After each plate had been blocked with 1% BSA in MDEM, 20000 cells/well were added to the well and incubated for 1 h. After the cells had been washed, the number of attached cells was assessed by crystal violet staining. Data are expressed as the mean ± SE of triplicate results. *$P < 0.01$ vs control.

We examined the amino acid sequence requirements of B133g for these activities using a set of alanine-substituted B133g peptides (Figure 6 and Table 2). The peptide in which the third Ile was substituted with Ala (B133g03) lost transition of UV absorption spectra on Congo Red staining. The first Asp-substituted peptide (B133g01) significantly reduced the absorption at 540 nm (Figure 6). The peptides substituted at the second Ser, sixth Tyr, seventh Phe, ninth Met, and eleventh Leu with Ala also reduced the absorption at 540 nm. The other Ala-substituted peptides retained the activity profile of B133g. These results suggest that the first Asp and third Ile residues provide a critical contribution for the amyloid-like fibril formation activity of B133g.

*Analysis of Amyloid-like Fibrils by Electron Microscopy*. We examined the amyloid-like fibrils of the alanine-substituted B133g peptides by negative staining electron microscopy (Figure 7). B133g exhibited typical amyloid-like fibrils. The B133g02, B133g06, B133g08, and B133g10 peptides exhibited thicker fibrils and the B133g09 and B133g11 peptides thinner filaments compared with those of B133g. The fiber density of B133g04, B133g06, B133g08, and B133g11 was lower while that of B133g10 higher than that of B133g. B133g05 and B133g07 formed fibers similar to those of B133g. In contrast, B133g01 and B133g03 did not form fibrils. These results are comparable with those of the Congo Red analysis and strongly suggest that the

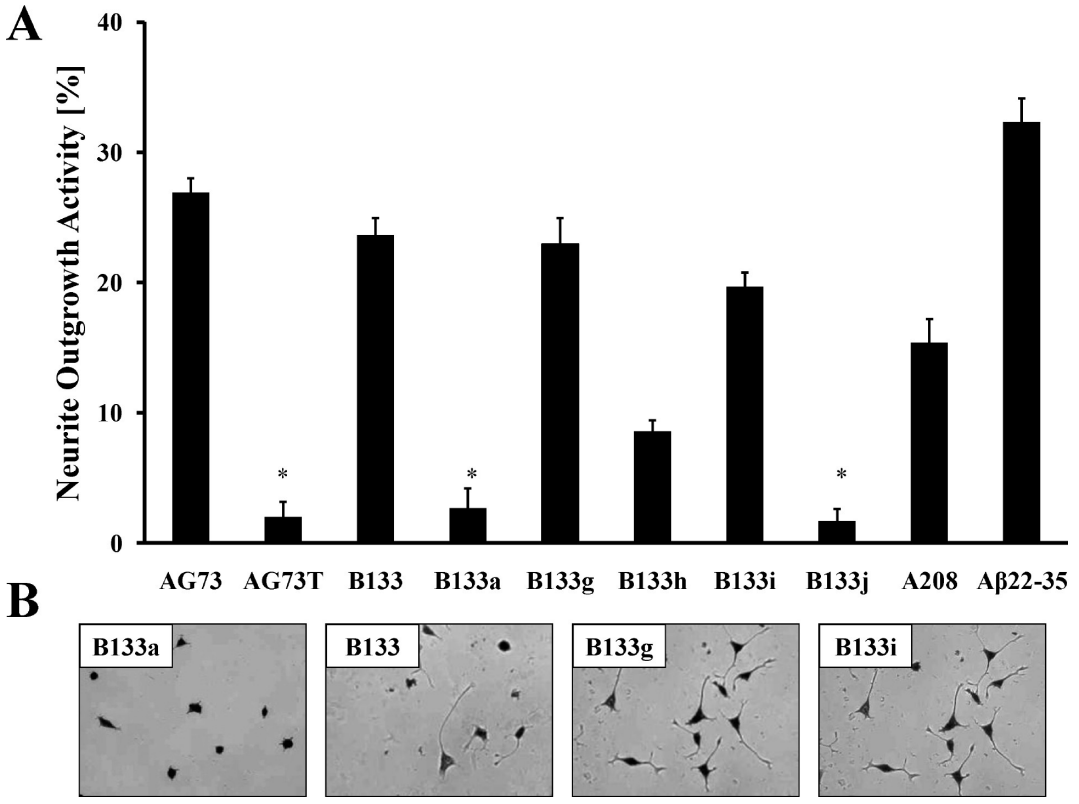


FIGURE 5: Neurite outgrowth of PC12 cells on peptides. (A) Fifty or ten micrograms of peptides was coated on 96-well plates. PC12 cells (5000 cells/well) were seeded in the plates. After a 24 h incubation, cells were fixed and stained. The percentage of PC12 cells with neurites was determined as described in Materials and Methods. AG73 was used as a positive control, and AG73T was used as a negative control. (B) The PC12 cells were cultured on various peptides for 24 h and then stained with crystal violet. Peptides were coated on 96-well plates. B133, A208, and A$\beta$22−35 at 50 $\mu$g/well and AG73, AG73T, B133g, B133h, and B133i at 10 $\mu$g/well. *$P < 0.01$ vs AG73.

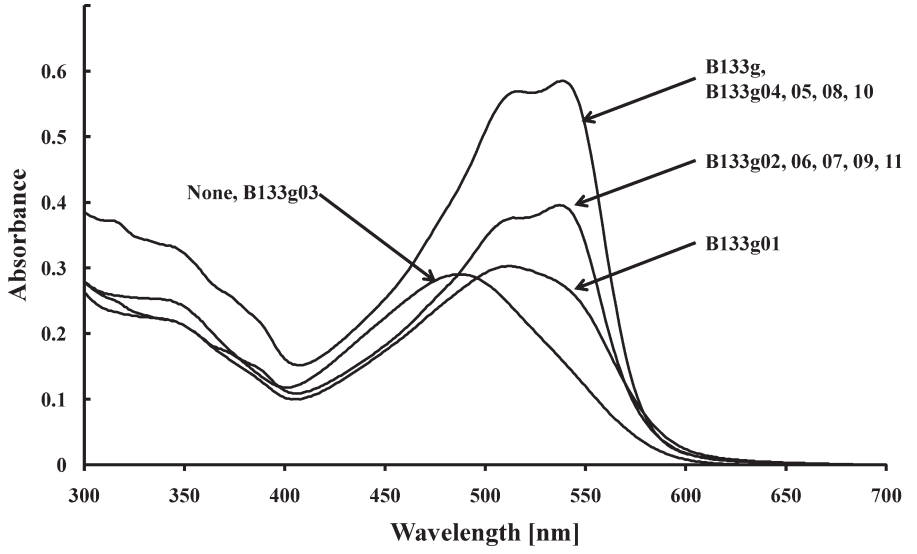


FIGURE 6: Absorption spectra of a Congo Red solution in the presence of peptides. Peptides dissolved in water (100 $\mu$L, 1.0 mg/mL) and a Congo Red solution (100 $\mu$L, 100 $\mu$M in PBS) were mixed with 800 $\mu$L of PBS (1.25×) and incubated for 24 h at room temperature. Absorption spectra were recorded from 300 to 700 nm.

first Asp and third Ile residues are critical for the self-assembly and amyloid-like fibril formation activity.

*Effect of Alanine-Substituted B133g Peptides on Cell Attachment*. We evaluated the cell attachment activity of the alanine-substituted B133g peptides using HT1080 cells (Figure 8). Cell attachment activities were significantly decreased in the peptide with alanine substituted at the first Asp and third Ile. The second Ser-substituted B133g peptide exhibited decreased cell attachment activity. The tenth Ser-substituted B133g peptide (B133g10) enhanced cell attachment activity. The other Ala-substituted peptides did not affect cell attachment activity. These results suggest that the first Asp residue and third Ile residue are important for cell attachment as well as for amyloid-like fibril formation.

*Effect of Alanine-Substituted B133 Peptides on Neurite Outgrowth*. We also evaluated the neurite outgrowth activity of

Table 2: Biological Activities of B133g and Its Alanine-Substituted Derivatives

| Peptide | Sequence | Congo red binding analysis[a] | Amyloid-like fibril formation | Cell attachment[b] (HT1080) | Neurite outgrowth[b] |
|---|---|---|---|---|---|
| B133g | DSITKYFQMSL | +++ | + | + | + |
| B133g01 | **A**SITKYFQMSL | + | − | − | − |
| B133g02 | D**A**ITKYFQMSL | ++ | + | + | + |
| B133g03 | DS**A**TKYFQMSL | − | − | − | + |
| B133g04 | DSI**A**KYFQMSL | +++ | + | + | + |
| B133g05 | DSIT**A**YFQMSL | +++ | + | + | + |
| B133g06 | DSITK**A**FQMSL | ++ | + | + | + |
| B133g07 | DSITKY**A**QMSL | ++ | + | + | + |
| B133g08 | DSITKYF**A**MSL | +++ | + | + | + |
| B133g09 | DSITKYFQ**A**SL | ++ | + | + | + |
| B133g10 | DSITKYFQM**A**L | +++ | + | + | + |
| B133g11 | DSITKYFQMS**A** | ++ | + | + | + |

[a]Peptides were incubated with a Congo Red solution, and the absorption spectrum at 540 nm was evaluated on the following subjective scale: +++, strong spectrum compared to that of B133; ++, spectrum comparable to that of B133; +, weak spectrum compared to that of B133; −, no shift in the absorption peak. [b]Attachment of HT1080 cells to peptides and neurite outgrowth of PC12 cells were scored on the following subjective scale: +, activity comparable to that on B133g; −, inactive.

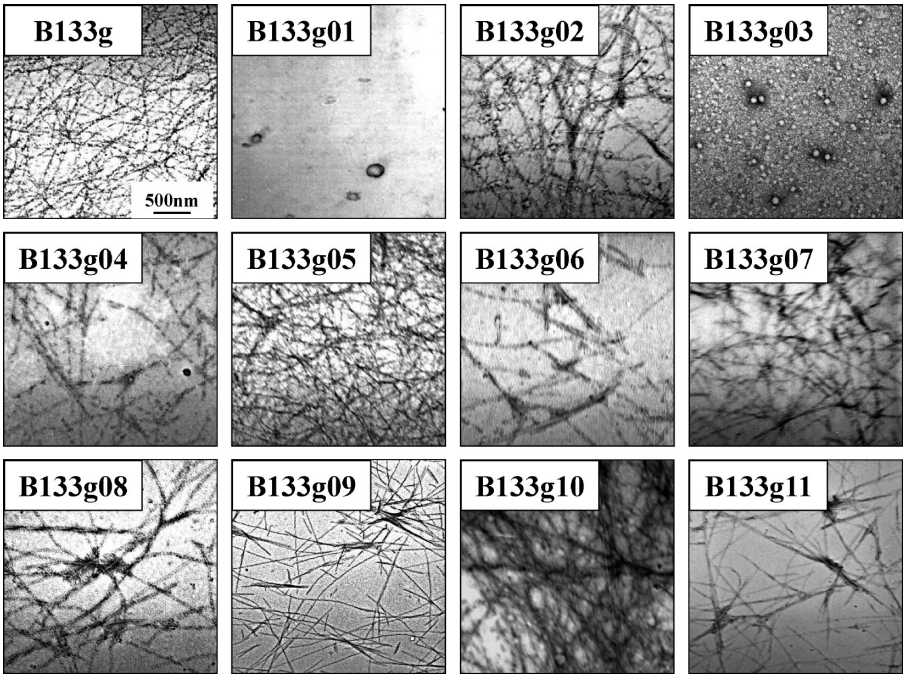


FIGURE 7: Electron micrograph of amyloid-like fibrils formed from peptides. A peptide solution (1 mg/mL) was diluted doubly with water and applied to a grid mesh with carbon-coated Formvar film. The specimen was then negatively stained with a 1.5% aqueous solution of uranyl acetate and observed using an electron microscope. The scale bar represents 500 nm.

the alanine-substituted B133g peptides (B133g01−11) (Figure 9). Neurite outgrowth of PC12 cells were not stimulated on B133g01. The other alanine-substituted peptides exhibited neurite outgrowth activity similar to that of B133g. Morphological differences were not observed among the peptides (data not shown). These results suggest that the first Asp residue is important for the neurite outgrowth activity as well as for amyloid-like fibril formation, but the third Ile residue is not important for neurite outgrowth activity.

## DISCUSSION

Amyloid fibril formation is generally related to diseases, including Alzheimer's disease, Parkinson's disease, type II diabetes, prion diseases, and systemic polyneuropathies (*6*, *7*). Although there have been many studies of amyloidogenesis mechanisms (*32*−*34*), the reports of the peptidic characteristics for amyloid fibril formation are limited. We previously reported five amyloidogenic peptides derived from laminin-111, including

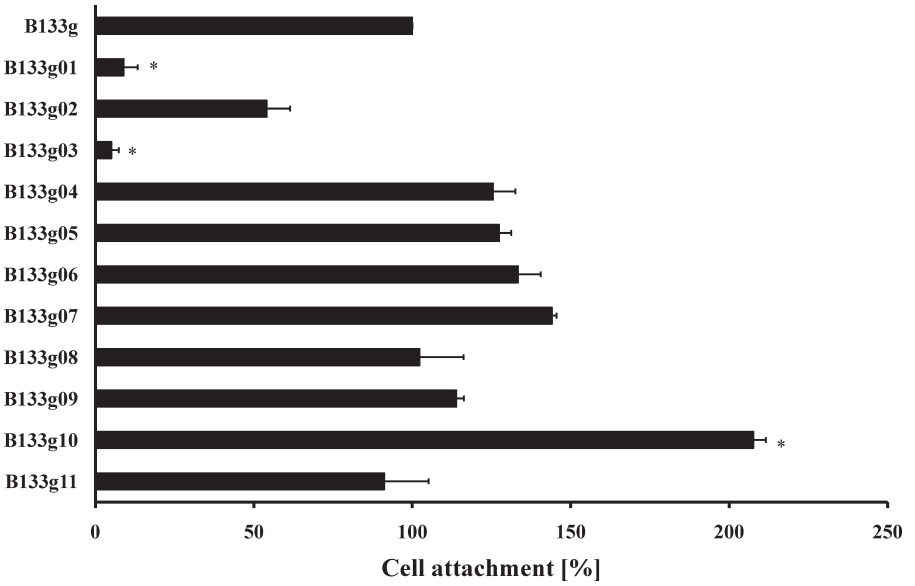


FIGURE 8: Cell attachment activity of B133g and its alanine-substituted peptides. Ninety-six-well plates were coated with various amounts of peptides, and HT-1080 cells were added. After a 1 h incubation, the number of attached cells was assessed by crystal violet staining. Data are expressed as means ± SE of triplicate results. AG73 and AG73T were used as positive and negative controls, respectively. *$P < 0.01$ vs B133g.

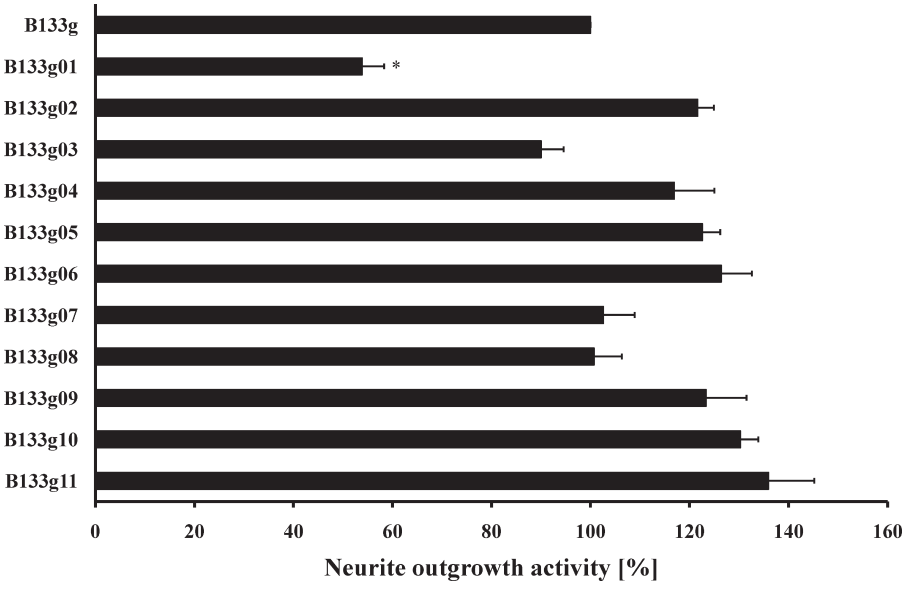


FIGURE 9: Neurite outgrowth of PC12 cells on B133g and its alanine-substituted peptides. Ten micrograms of peptides was coated on 96-well plates. PC12 cells (5000 cells/well) were seeded in the plates. After a 24 h incubation, cells were fixed and stained. The percentage of PC12 cells with neurites was determined as described in Materials and Methods. AG73 was used as a positive control and AG73T as a negative control. *$P < 0.01$ vs B133g.

peptides A119, A208, AG97, B133, and B160. These peptides also promote cell attachment, and the Arg-Gly-Asp (RGD) sequence-conjugated amyloidogenic peptide has potential as a biomaterial (*5*, *31*, *35*). Here, we focused on the amyloidogenic peptide B133, which promotes both integrin α2$\beta$1-mediated cell attachment and a heparin-dependent cell attachment. The N- and C-terminal amino acid deletion of the B133 peptide separates the functions; the N-terminal deletion peptide promotes only integrin-mediated cell attachment, and the C-terminal deletion peptide shows only heparin-dependent cell attachment and amyloidogenesis. The C-terminal Asp-deleted peptide B133g has strong absorption at 540 nm in Congo Red staining analysis, and the absorbance was higher than that of B133 and A$\beta$22−35. The observation of polarized microscopy and electron microscopy of B133g also strongly suggests that the peptide forms amyloid-like fibrils. Amyloid fibrils are known to be self-cohesive and insoluble, and its structure is built up by stacking $\beta$ strands to form a cross-$\beta$ structure (*11*, *12*). The fibrils are not dependent on the hydrophobicity of the peptides, but on specific interactions between peptides. For example, amyloid $\beta$ peptide(1−42) in its natural structure forms self-assembled insoluble fibrils, while its *O*-acyl isopeptide structure at $Gly^{25}$-$Ser^{26}$ remains soluble and does not form fibrils (*36*). The amyloidogenesis of a peptide depends on the primary structure, and an amino acid residue replacement or deletion can "switch" between amyloid-forming and -degrading. In our results, the N-terminal Asp and the third Ile of peptide B133 are important for the amyloid-like fibril structure. Several studies on amyloid fibril formation suggest that

the interaction of specific amino acid residues contributes to the formation and stabilization of the amyloid fibrils (*12*, *37*−*39*). Electrostatic interaction by basic and acidic amino acids is suggested to be critical for fibril formation and/or stabilization of fibrils (*12*, *39*). It has also been proposed that aromatic amino acids are an important property for amyloid fibrils (*38*). The sixth Tyr-substituted (B133g06) and the seventh Phe-substituted (B133g07) B133g peptides had decreased the UV absorption at 540 nm in Congo Red staining analyses but did not show a significant difference in the formation of amyloid-like fibrils in this study. Aromatic amino acids thus may not be essential for the B133 amyloid fibril formation but may accelerate fibril formation. Although the second Ser-substituted (B133g02), ninth Met-substituted (B133g09), and the eleventh Leu-substituted (B133g11) peptides also decreased the UV absorption at 540 nm in Congo Red staining analyses (Figure 6), significant differences in fiber configuration were not observed by electron microscopy (Figure 7). Since amyloid-like fibrils are composed of a cross-$\beta$ structure, amyloid-like fibril formation requires preservation of the $\beta$ sheet structure and self-cohesive properties. Circular dichroism (CD) spectrum analysis indicated that B133g03 preserved a $\beta$ sheet structure of B133g but B133g01 did not (data not shown). In this study, it is not clear whether the density and/or size of fibrils may be dependent on the hydrophobicity and polarity of the side chains. Taken together, we conclude that both hydrophobic and electrostatic interactions may be necessary for peptide amyloid-like fibril formation.

Here, we showed that cell attachment of N-terminal truncated peptides of B133 strongly correlates with amyloid-like fibril formation. Further, cell attachment is mediated by syndecan specifically. When a protein (peptide) attaches to cells, there are two mechanisms; one is mediated by receptors, which is protein (peptide)-specific, and the other is nonspecific attachment to a peptidyl scaffold. We reported that the amyloid-like fibrils of A208 are useful for the generation of cell culture scaffolds, and that RGD motif-conjugated A208 peptides recognize both the IKVAV receptor and integrin $\alpha v\beta 3$ and are applicable as a cell-adhesive biomaterial (*35*). B133g is also an amyloidogenic peptide and promotes syndecan-mediated cell attachment. The B133g peptide is expected to be useful as a multifunctional biomaterial and as a bioadhesive/scaffold for tissue engineering.

Generally, it is thought that $\beta$-amyloid protein (A$\beta$) has a neurotoxic effect (*25*, *40*). We found that A$\beta$22−35, when coated on a plastic plate as a substrate, promoted syndecan-mediated cell attachment and neurite outgrowth with PC12 cells (Figures 4 and 5). In this study, B133g and its derivatives have neurite outgrowth activities at low concentrations when compared to the B133 peptide. The alanine scan assay identified the first Asp as an essential residue. For neurite outgrowth activity, signaling into the cells mediated by receptors is needed. Peptide B133g promoted a syndecan-mediated cell attachment, but B133g03 did not promote cell attachment or form amyloid-like fibrils; however, the peptide did exhibit neurite outgrowth activity. These data suggest that other receptor(s) may be involved in peptide-mediated neurite outgrowth. Recently, the existence of functional amyloids that are low in toxicity and stored as amyloid fibrils (*41*) in the pituitary and in other organs has been reported. The amyloidogenic peptide B133g and its derivatives are weakly toxic, and their amyloidogenesis and neurite outgrowth activities can be useful in the treatment of diseases due to neurite damage. In addition, laminin and certain degraded fragments interact with A$\beta$, inhibit amyloid fibril formation, and are present in Alzheimer's plaques (*42*). Many bioactive peptides have been identified from various proteins, including laminins (*43*−*45*), fibronectins (*46*), and collagens (*47*). Some of the peptides may form amyloid-like fibrils, but that has not been extensively studied yet. B133g and the derivatives have potential for use as a model amyloidogenic peptide for amyloid-like fibrils.

In this study, we identified essential residues in the amyloidogenic peptide B133g on syndecan-mediated cell attachment, neurite outgrowth, and amyloid-like fibril formation. The N-terminal Asp residue is critical for the B133g biological and fibril-forming activities, and the third Ile is important for fibril formation. These results are important for understanding the relation between amyloid-like fibril formation and biological functions and are useful for the investigation of amyloidogenesis in vivo and creation of biomaterials and therapeutic drugs.

## REFERENCES


1. Cooper, J. H. (1974) Selective amyloid staining as a function of amyloid composition and structure. Histochemical analysis of the alkaline Congo red, standardized toluidine blue, and iodine methods. *Lab. Invest. 31*, 232–238.
2. Azriel, R., and Gazit, E. (2001) Analysis of the minimal amyloid-forming fragment of the islet amyloid polypeptide. An experimental support for the key role of the phenylalanine residue in amyloid formation. *J. Biol. Chem. 276*, 34156–34161.
3. Klunk, W. E., Jacob, R. F., and Mason, R. P. (1999) Quantifying amyloid $\beta$-peptide (A$\beta$) aggregation using the Congo red-A$\beta$ (CR-a$\beta$) spectrophotometric assay. *Anal. Biochem. 266*, 66–76.
4. Yamada, M., Kadoya, Y., Kasai, S., Kato, K., Mochizuki, M., Nishi, N., Watanabe, N., Kleinman, H. K., Yamada, Y., and Nomizu, M. (2002) Ile-Lys-Val-Ala-Val (IKVAV)-containing laminin $\alpha$1 chain peptides form amyloid-like fibrils. *FEBS Lett. 530*, 48–52.
5. Kasai, S., Urushibata, S., Hozumi, K., Yokoyama, F., Ichikawa, N., Kadoya, Y., Nishi, N., Watanabe, N., Yamada, Y., and Nomizu, M. (2007) Identification of multiple amyloidogenic sequences in laminin-1. *Biochemistry 46*, 3966–3974.
6. Kelly, J. W. (1998) The alternative conformations of amyloidogenic proteins and their multi-step assembly pathways. *Curr. Opin. Struct. Biol. 8*, 101–106.
7. Rochet, J. C., and Lansbury, P. T., Jr. (2000) Amyloid fibrillogenesis: Themes and variations. *Curr. Opin. Struct. Biol. 10*, 60–68.
8. Brange, J., Andersen, L., Laursen, E. D., Meyn, G., and Rasmussen, E. (1997) Toward understanding insulin fibrillation. *J. Pharm. Sci. 86*, 517–525.
9. Guijarro, J. I., Sunde, M., Jones, J. A., Campbell, I. D., and Dobson, C. M. (1998) Amyloid fibril formation by an SH3 domain. *Proc. Natl. Acad. Sci. U.S.A. 95*, 4224–4228.
10. Ohnishi, S., Koide, A., and Koide, S. (2000) Solution conformation and amyloid-like fibril formation of a polar peptide derived from a $\beta$-hairpin in the OspA single-layer $\beta$-sheet. *J. Mol. Biol. 301*, 477–489.
11. Sipe, J. D., and Cohen, A. S. (2000) Review: History of the amyloid fibril. *J. Struct. Biol. 130*, 88–98.
12. Fraser, P. E., McLachlan, D. R., Surewicz, W. K., Mizzen, C. A., Snow, A. D., Nguyen, J. T., and Kirschner, D. A. (1994) Conformation and fibrillogenesis of Alzheimer A$\beta$ peptides with selected substitution of charged residues. *J. Mol. Biol. 244*, 64–73.
13. Colognato, H., and Yurchenco, P. D. (2000) Form and function: The laminin family of heterotrimers. *Dev. Dyn. 218*, 213–234.
14. Kleinman, H. K., Weeks, B. S., Cannon, F. B., Sweeney, T. M., Sephel, G. C., Clement, B., Zain, M., Olson, M. O., Jucker, M., and Burrous, B. A. (1991) Identification of a 110-kDa nonintegrin cell surface laminin-binding protein which recognizes an A chain neurite-promoting peptide. *Arch. Biochem. Biophys. 290*, 320–325.
15. Narindrasorasak, S., Lowery, D. E., Altman, R. A., Gonzalez-DeWhitt, P. A., Greenberg, B. D., and Kisilevsky, R. (1992) Characterization of high affinity binding between laminin and Alzheimer's disease amyloid precursor proteins. *Lab. Invest. 67*, 643–652.
16. Kibbey, M. C., Jucker, M., Weeks, B. S., Neve, R. L., Van Nostrand, W. E., and Kleinman, H. K. (1993) $\beta$-Amyloid precursor protein binds to the neurite-promoting IKVAV site of laminin. *Proc. Natl. Acad. Sci. U.S.A. 90*, 10150–10153.
17. Katagiri, F., Ohga, Y., Takeyama, K., Hozumi, K., Kikkawa, Y., Kadoya, Y., and Nomizu, M. (2010) B133 (DSITKYFQMSLE), a laminin $\alpha$1 derived peptide, contains distinct core sequences for the

integrin α2β1-mediated cell adhesion and for the amyloid-like fibril formation. *Arch. Biochem. Biophys.* (in press).
18. Nomizu, M., Kuratomi, Y., Malinda, K. M., Song, S. Y., Miyoshi, K., Otaka, A., Powell, S. K., Hoffman, M. P., Kleinman, H. K., and Yamada, Y. (1998) Cell binding sequences in mouse laminin α1 chain. *J. Biol. Chem. 273*, 32491–32499.
19. Greene, L. A., and Tischler, A. S. (1976) Establishment of a noradrenergic clonal line of rat adrenal pheochromocytoma cells which respond to nerve growth factor. *Proc. Natl. Acad. Sci. U.S.A. 73*, 2424–2428.
20. Hozumi, K., Suzuki, N., Nielsen, P. K., Nomizu, M., and Yamada, Y. (2006) Laminin α1 chain LG4 module promotes cell attachment through syndecans and cell spreading through integrin α2β1. *J. Biol. Chem. 281*, 32929–32940.
21. Liu, W., Litwack, E. D., Stanley, M. J., Langford, J. K., Lander, A. D., and Sanderson, R. D. (1998) Heparan sulfate proteoglycans as adhesive and anti-invasive molecules. Syndecans and glypican have distinct functions. *J. Biol. Chem. 273*, 22825–22832.
22. Langford, J. K., Stanley, M. J., Cao, D., and Sanderson, R. D. (1998) Multiple heparan sulfate chains are required for optimal syndecan-1 function. *J. Biol. Chem. 273*, 29965–29971.
23. Nomizu, M., Kuratomi, Y., Ponce, M. L., Song, S. Y., Miyoshi, K., Otaka, A., Powell, S. K., Hoffman, M. P., Kleinman, H. K., and Yamada, Y. (2000) Cell adhesive sequences in mouse laminin β1 chain. *Arch. Biochem. Biophys. 378*, 311–320.
24. Tashiro, K., Sephel, G. C., Weeks, B., Sasaki, M., Martin, G. R., Kleinman, H. K., and Yamada, Y. (1989) A synthetic peptide containing the IKVAV sequence from the A chain of laminin mediates cell attachment, migration, and neurite outgrowth. *J. Biol. Chem. 264*, 16174–16182.
25. Takadera, T., Sakura, N., Mohri, T., and Hashimoto, T. (1993) Toxic effect of a β-amyloid peptide (β 22−35) on the hippocampal neuron and its prevention. *Neurosci. Lett. 161*, 41–44.
26. Nomizu, M., Kim, W. H., Yamamura, K., Utani, A., Song, S. Y., Otaka, A., Roller, P. P., Kleinman, H. K., and Yamada, Y. (1995) Identification of cell binding sites in the laminin α1 chain carboxyl-terminal globular domain by systematic screening of synthetic peptides. *J. Biol. Chem. 270*, 20583–20590.
27. Hoffman, M. P., Nomizu, M., Roque, E., Lee, S., Jung, D. W., Yamada, Y., and Kleinman, H. K. (1998) Laminin-1 and laminin-2 G-domain synthetic peptides bind syndecan-1 and are involved in acinar formation of a human submandibular gland cell line. *J. Biol. Chem. 273*, 28633–28641.
28. Hoffman, M. P., Engbring, J. A., Nielsen, P. K., Vargas, J., Steinberg, Z., Karmand, A. J., Nomizu, M., Yamada, Y., and Kleinman, H. K. (2001) Cell type-specific differences in glycosaminoglycans modulate the biological activity of a heparin-binding peptide (RKRLQVQLSIRT) from the G domain of the laminin α1 chain. *J. Biol. Chem. 276*, 22077–22085.
29. Suzuki, N., Ichikawa, N., Kasai, S., Yamada, M., Nishi, N., Morioka, H., Yamashita, H., Kitagawa, Y., Utani, A., Hoffman, M. P., and Nomizu, M. (2003) Syndecan binding sites in the laminin α1 chain G domain. *Biochemistry 42*, 12625–12633.
30. Suzuki, N., Nakatsuka, H., Mochizuki, M., Nishi, N., Kadoya, Y., Utani, A., Oishi, S., Fujii, N., Kleinman, H. K., and Nomizu, M. (2003) Biological activities of homologous loop regions in the laminin α chain G domains. *J. Biol. Chem. 278*, 45697–45705.
31. Ohga, Y., Katagiri, F., Takeyama, K., Hozumi, K., Kikkawa, Y., Nishi, N., and Nomizu, M. (2009) Design and activity of multifunctional fibrils using receptor-specific small peptides. *Biomaterials 30*, 6731–6738.
32. Jean, L., Lee, C. F., Lee, C., Shaw, M., and Vaux, D. J. (2010) Competing discrete interfacial effects are critical for amyloidogenesis. *FASEB J. 24*, 309–317.
33. Pop, V., Head, E., Berchtold, N. C., Glabe, C. G., Studzinski, C. M., Weidner, A. M., Murphy, M. P., and Cotman, C. W. (2010) Aβ aggregation profiles and shifts in APP processing favor amyloidogenesis in canines. *Neurobiol. Aging* (in press).
34. Marks, N., and Berg, M. J. (2010) BACE and γ-secretase characterization and their sorting as therapeutic targets to reduce amyloidogenesis. *Neurochem. Res. 35*, 181–210.
35. Kasai, S., Ohga, Y., Mochizuki, M., Nishi, N., Kadoya, Y., and Nomizu, M. (2004) Multifunctional peptide fibrils for biomedical materials. *Biopolymers 76*, 27–33.
36. Sohma, Y., Hayashi, Y., Kimura, M., Chiyomori, Y., Taniguchi, A., Sasaki, M., Kimura, T., and Kiso, Y. (2005) The 'O-acyl isopeptide method' for the synthesis of difficult sequence-containing peptides: Application to the synthesis of Alzheimer's disease-related amyloid β peptide (Aβ) 1−42. *J. Pept. Sci. 11*, 441–451.
37. Hilbich, C., Kisters-Woike, B., Reed, J., Masters, C. L., and Beyreuther, K. (1992) Substitutions of hydrophobic amino acids reduce the amyloidogenicity of Alzheimer's disease β A4 peptides. *J. Mol. Biol. 228*, 460–473.
38. Reches, M., Porat, Y., and Gazit, E. (2002) Amyloid fibril formation by pentapeptide and tetrapeptide fragments of human calcitonin. *J. Biol. Chem. 277*, 35475–35480.
39. Tjernberg, L., Hosia, W., Bark, N., Thyberg, J., and Johansson, J. (2002) Charge attraction and β propensity are necessary for amyloid fibril formation from tetrapeptides. *J. Biol. Chem. 277*, 43243–43246.
40. Koo, E. H., Park, L., and Selkoe, D. J. (1993) Amyloid β-protein as a substrate interacts with extracellular matrix to promote neurite outgrowth. *Proc. Natl. Acad. Sci. U.S.A. 90*, 4748–4752.
41. Maji, S. K., Perrin, M. H., Sawaya, M. R., Jessberger, S., Vadodaria, K., Rissman, R. A., Singru, P. S., Nilsson, K. P., Simon, R., Schubert, D., Eisenberg, D., Rivier, J., Sawchenko, P., Vale, W., and Riek, R. (2009) Functional amyloids as natural storage of peptide hormones in pituitary secretory granules. *Science 325*, 328–332.
42. Castillo, G. M., Lukito, W., Peskind, E., Raskind, M., Kirschner, D. A., Yee, A. G., and Snow, A. D. (2000) Laminin inhibition of β-amyloid protein (Aβ) fibrillogenesis and identification of an Aβ binding site localized to the globular domain repeats on the laminin a chain. *J. Neurosci. Res. 62*, 451–462.
43. Suzuki, N., Yokoyama, F., and Nomizu, M. (2005) Functional sites in the laminin α chains. *Connect. Tissue Res. 46*, 142–152.
44. Urushibata, S., Katagiri, F., Takaki, S., Yamada, Y., Fujimori, C., Hozumi, K., Kikkawa, Y., Kadoya, Y., and Nomizu, M. (2009) Biologically active sequences in the mouse laminin α3 chain G domain. *Biochemistry 48*, 10522–10532.
45. Urushibata, S., Hozumi, K., Ishikawa, M., Katagiri, F., Kikkawa, Y., and Nomizu, M. (2010) Identification of biologically active sequences in the laminin α2 chain G domain. *Arch. Biochem. Biophys. 497*, 43–54.
46. Ruoslahti, E., and Pierschbacher, M. D. (1987) New perspectives in cell adhesion: RGD and integrins. *Science 238*, 491–497.
47. Miles, A. J., Knutson, J. R., Skubitz, A. P., Furcht, L. T., McCarthy, J. B., and Fields, G. B. (1995) A peptide model of basement membrane collagen α1 (IV) 531−543 binds the α3β1 integrin. *J. Biol. Chem. 270*, 29047–29050.